THE EXPERIMENTAL RESEARCH OF COMPRESSORS IN A PET BOTTLES FACTORY FOR SOFT DRINKS

Laurențiu LIPAN[1], Sorin DIMITRIU[2]

In this paper, the authors present the results of investigations performed on the operation of the compressor station of a PET bottle factory for soft drinks. Both thermal and electrical measurements were performed. The aim was to investigate energy consumption and determine the energy performance indicators of compressors. The aim was also to investigate the quality of the electric power supply to the compressor station. Based on the results of the measurements, conclusions were drawn on increasing the energy efficiency of the operation of the compressor station and improving the quality of the electricity with which the compressors are supplied.

Keywords: compressors, experimental research, compressor energetics, energy consumption control strategy

1. Introduction

In the soft drink industry, more than 70% of the packaging used for bottling is made of plastic, polyethylene terephthalate (PET) being the preferred material, before aluminum and glass. The advantages of using PET for bottling are strength, light weight, and recyclability. To obtain plastic bottles, PET must first go through a polymerization process, to create long molecular chains. Once the PET has been polymerized, the process of obtaining the bottle, which comprises several stages, follows (Fig. 1):

- a cylindrical tube (parison) with a certain length is first made by extrusion.
- the heated parison is inserted inside a mold that has the shape of the container and by blowing air with high pressure, it stretches and takes the shape of the mold.
- the formed plastic bottle is quickly cooled and removed from the mold.

The essential element that determines the obtaining of a product of suitable quality is the compressed air that the blower introduces inside the mold, for the deformation of the parison.

[1] Lecturer, Dept. of Power Eng. Systems, University POLITEHNICA of Bucharest, Romania, e-mail: laurentiulipan@gmail.com

[2] Assoc. Prof., Dept. of Eng. Thermodynamics, Thermal engines, Thermal and refrigerating equipment, University POLITEHNICA of Bucharest, Romania, e-mail: dimitriu47@yahoo.com

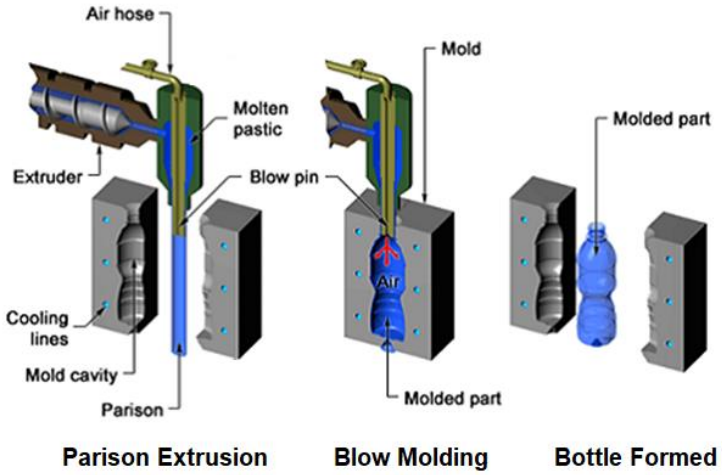

Fig. 1 Process of PET bottle manufacturing (Source: PMB PlasticBoTTLE^{TM} [1])

Therefore, PET beverage bottle mills have a high-pressure compressor station, which must supply compressed air continuously at the required constant pressure and a flow continuously correlated with the rate of production of the bottles. These requirements are essential to obtain products of appropriate quality. Traditionally, plastic bottle factories use electrically operated piston compressors capable of supplying compressed air with a pressure of 40 ... 50 bar, equipped with regulation and control systems that ensure, on the one hand, a constant pressure of air, and on the other hand, a variable flow, according to production needs, in conditions of maximum energy efficiency [2], [3].

In the present paper, the authors present the experimental results obtained by studying the operation of the compressor station of a section to produce PET bottles, within a soft drink factory.

2. Overview

The studied compressor station has in its composition four compressors of 40 bar from the CE series, produced by "Ateliers Francois SA - Belgium" (Fig. 2) for the supply of compressed air to the blowers for bottles made of thermoplastic material (PET). The technical characteristics of the compressors are presented in Table 1.

Table 1

Technical characteristics of compressors

Type	No. pcs.	Nominal pressure [bar]	Nominal flow [m^3/min]	Rated power [kW]	Nominal speed [rpm]
CE 46 B	1	40	22,0	250	500
CE 68 B	2	40	43.3	450	520
CE 680 B	1	40	53.0	550	540

Fig. 2 The compressors station of PET bottles plant (Author's image).

High pressure AF compressors (40 bar) are specially designed for the blowing of PET bottles. The construction of the compressors is cross headed, in three stages grouped in two lines of cylinders arranged in L. Compression stage I forms the vertical line and stages II and III, the horizontal line (fig.3). Between the compression stages and finally, the air is cooled with water. The compressor cylinders are also cooled with water. The cooling water is circulated by a closed-circuit circulation pump, the heat taken from the compressor being evacuated by means of external cooling coils, cooled by atmospheric air. The pistons of the three stages are without lubrication, with Teflon segments, the pressure lubrication being used only for the bearings of the crankshaft and the crosshead guides. This prevents the oil entrained by the compressed air from entering the PET bottle blower.

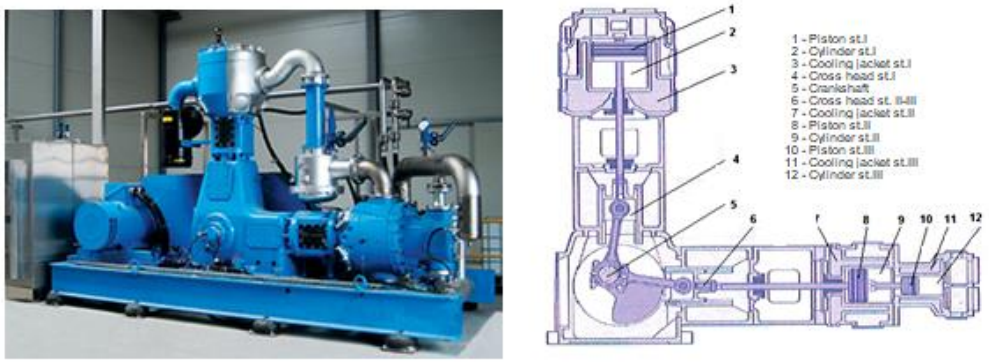

Fig. 3 Compressor AF CE 68 B (40 bar; 43.3 m^3/h) (Source: AF Compressors [4]).

The electric motors are of three-phase alternating current, the transmission to the compressor being made through the belts. The compressor is equipped with an intelligent flow control system consisting of a pneumatic locking device in the "open" position of the suction valves of stage I. The cylinder of stage I is double acting, the piston having both sides active (Fig. 2). If the compressor discharge pressure increases above the set pressure of 40 bar, it is ordered to introduce compressed air inside an execution element, consisting of a small piston cylinder, which inserts a fork through the holes of the suction valve of the lower part of the cylinder, blocking it in an "open" position. Decommissioning the lower part of the cylinder has the effect of lowering the compressor flow to approx. 50% and obviously the discharge pressure will decrease, causing the fork to retract and the lower part of the cylinder to resume operation. This ensures the supply of compressed air for use with a constant pressure of 40 bar, and flow in the range of 50% ... 100% of the nominal flow. If the consumer requests a flow rate even less than 50% of the nominal flow rate, the lower suction valve shall be kept permanently open and the upper suction valve, which is fitted with a similar actuator, shall lock periodically in "open" position, depending on the tendency of the discharge pressure, to increase or decrease, ensuring a constant discharge pressure for any flow within the limit of 0% ... 50% of the nominal flow. This control method ensures a constant discharge pressure, at the set value, for any flow in the control range 0% ... 50% and 50% ... 100% of the nominal flow. The compression ratios on each stage are self-adjusting (Table 2), as the first stage cylinder operates with double effect (100% flow) or single effect (50% flow).

The power electronics that control the electric drive motor ensure its constant speed at any load regime and the control of the idle / load state.

Table 2

Compression ratios when operating changes

Operating mode	Compression ratios		
	Stage I	Stage II	Stage III
100 % - double effect	5.20	3.11	2.47
50 % - simple effect	2.82	3.27	4.34

3. The piston compressor energetics.

In the case of multi-stage compressors, the total mechanical work is the sum of the mechanical works corresponding to each stage. The optimum conditions for carrying out the process, which lead to a minimum of mechanical compression work, require that the compression ratios be equal at all stages, and after each intermediate cooler the air temperature be returned to the suction temperature at the first stage. According to these conditions the total mechanical work of real compression is given by the relation:

$$|l_r| = z\frac{n}{n-1}R\,T_a\left[\left(\sigma^z\frac{p_r}{p_a}\right)^{\frac{n-1}{n\,z}}-1\right] \quad [\text{J/kg}] \tag{1}$$

where: p_a is the suction pressure, p_r is the discharge pressure, z is the number of compression stages, n is the polytropic exponent of the compression process, and σ is the coefficient of losses by throttling in the compressor valves [5]. The pressure losses in the compressor valves are considered by the throttling coefficients at suction ψ_a and at discharge ψ_r respectively:

$$\psi_a = \frac{\Delta p_a}{p_a};\quad \psi_r = \frac{\Delta p_r}{p_r} \tag{2}$$

resulting in the expression, the compression ratio on compressor stage:

$$\frac{p_r'}{p_a'} = \frac{p_r+\Delta p_r}{p_a-\Delta p_a} = \frac{p_r}{p_a}\frac{1+\psi_r}{1-\psi_a} = \sigma\frac{p_r}{p_a} \tag{3}$$

where the value of the throttle coefficient in the valve, in the case of air compressors with sealing ring valves, is in the range σ = 1.15 ... 1.20 [6]:

The mass flow of the compressor is expressed:

$$\dot{m} = \frac{\dot{V}_a\,\rho_a}{60} = \frac{10^5}{60}\frac{p_a\,\dot{V}_a}{R\,T_a} = \quad [\text{kg/s}] \tag{4}$$

where $\dot{V}_a$ [m^3/min] is the flow, ρ_a [kg/m^3] the air density, and p_a [bar] the air pressure respectively, at suction conditions.

The power required for the real compression process has the expression:

$$P_r = \dot{m}\,|l_r|\cdot 10^{-3} = 1.67\cdot z\frac{n}{n-1}p_a\,\dot{V}_a\left[\left(\sigma^z\frac{p_r}{p_a}\right)^{\frac{n-1}{n\,z}}-1\right] \quad [\text{kW}] \tag{5}$$

and for σ = 1(without losses by throttling in valves), the theoretical power results:

$$P_t = 1.67\cdot z\frac{n}{n-1}p_a\,\dot{V}_a\left[\left(\frac{p_r}{p_a}\right)^{\frac{n-1}{n\,z}}-1\right] \quad [\text{kW}] \tag{6}$$

The power consumed in addition, due to the throttling in the distribution system, can be calculated with the relation:

$$P_{lam} = P_r - P_t = 1.67\cdot z\frac{n}{n-1}p_a\,\dot{V}_a\left(\sigma^{\frac{n-1}{n}}-1\right)\left(\frac{p_r}{p_a}\right)^{\frac{n-1}{n\,z}} \quad [\text{kW}] \tag{7}$$

The difference between the rated power at the compressor shaft P_{Na}[kW] and the theoretical power P_{Nt} [kW], corresponding to the rated flow $\dot{V}_{aN}$ [m^3/min], represents the compressor losses: mechanical losses and losses due to throttling in the distribution system:

$$P_{pierd} = P_{Na} - P_{Nt} = P_{mec} + P_{Nlam} \quad [\text{kW}] \tag{8}$$

wherein P_{Nlam} represents the losses introduced by the throttling process:

$$P_{lam,N} = 1.67 \cdot z \frac{n}{n-1} p_a \dot{V}_{aN} \left(\sigma^{\frac{n-1}{n}} - 1 \right) \left(\frac{p_r}{p_a} \right)^{\frac{n-1}{n\,z}} \quad [\text{kW}] \tag{9}$$

It can be considered that the mechanical losses of the machine, at constant speed, do not depend on the flow and can be determined from the power balance at rated speed:

$$P_{mec} = P_{Na} - P_{Nt} - P_{Nlam} \quad [\text{kW}] \tag{10}$$

These losses determine the nominal efficiency of the machine:

$$\eta_N = \frac{P_{Nt}}{P_{Na}} 100 = \frac{P_t}{P_{Nt} + P_{mec} + P_{lam}} 100 \quad [\%] \tag{11}$$

For a certain flow, different from the nominal one, the efficiency will be expressed:

$$\eta = \frac{P_t}{P_a} 100 = \frac{P_t}{P_t + P_{mec} + P_{lam}} 100 \quad [\%] \tag{12}$$

and is a function of the realized flow, being within the limits $\eta = 0 \ldots \eta_N$. It turns out that for compressors that run continuously at constant speed, the efficiency decreases with the flow of the machine. Obviously, at idle the efficiency is zero, as the compressor consumes energy only to cover internal losses. Table 3 presents, according to the above relationships, the characteristic sizes, and losses for the four compressors at rated load:

Table 3

Compressor parameters and efficiency at rated load

No.	Parameter	Symbol.	Unit	Compressor type			
				AF1 CE 68B	AF2 CE 680B	AF3 CE 68B	AF4 CE 46B
1	Rated flow	$\dot{V}_N$	m^3/min	43.3	53.3	43.3	22.0
2	Nominal speed	n_r	rpm	520.0	540.0	520.0	500.0
3	Rated power	P_N	kW	450.0	550.0	450.0	250.0
4	Theoretical power	P_{Nt}	kW	323.1	397.7	323.1	164.1
5	Throttling loses	P_{Nlam}	kW	59.0	72.6	59.0	29.3
6	Mechanical loses	P_{Nm}	kW	68.0	79.8	68.0	55.9

7	Compressor efficiency	η_{Nc}	%	71.8	72.3	71.8	65.7
8	El. motor efficiency	η_m	%	92.0	92.0	92.0	92.0
9	Total efficiency	η_{Nmc}	%	66.1	66.5	66.1	60.4

4. Compressor operation monitoring results

The operation of the compressors was monitored by measuring and recording the electrical power consumed, the air flows produced and the voltage and current characteristics at the general supply board of the compressor station. The results of the measurements are presented in Figs. 4 ... 7.

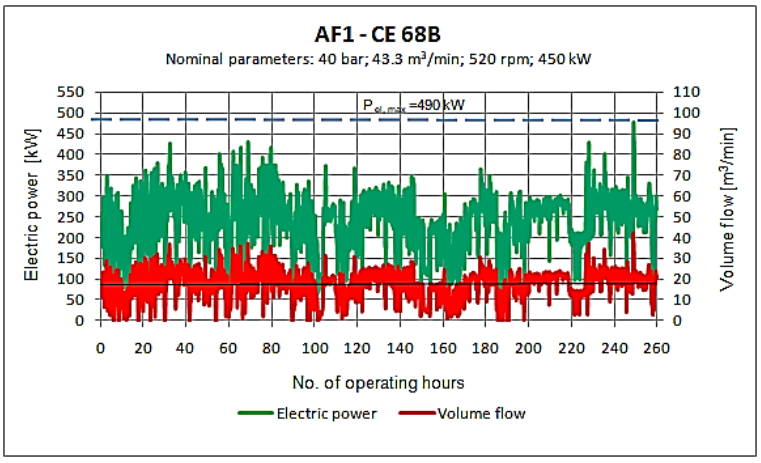

Fig. 4 Electric power and volume flow for compressor AF1-CE 68B

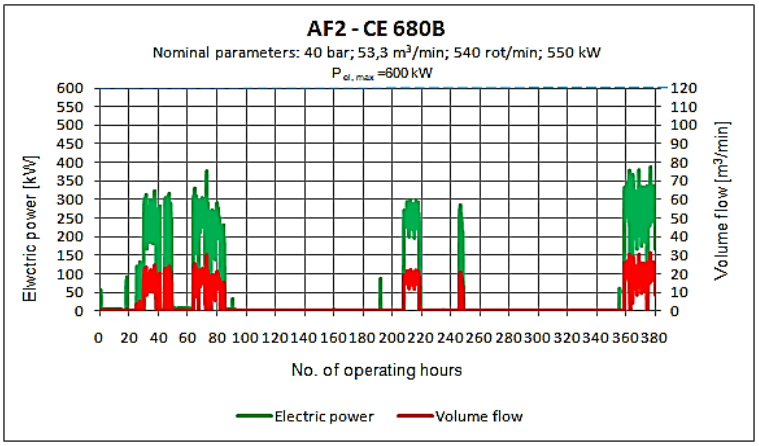

Fig. 5 Electric power and volume flow for compressor AF2-CE 680B

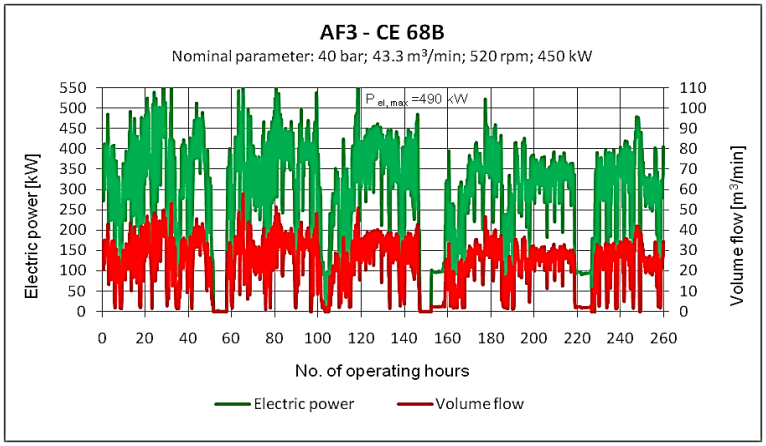

Fig. 6 Electric power and volume flow for compressor AF3-CE 68B

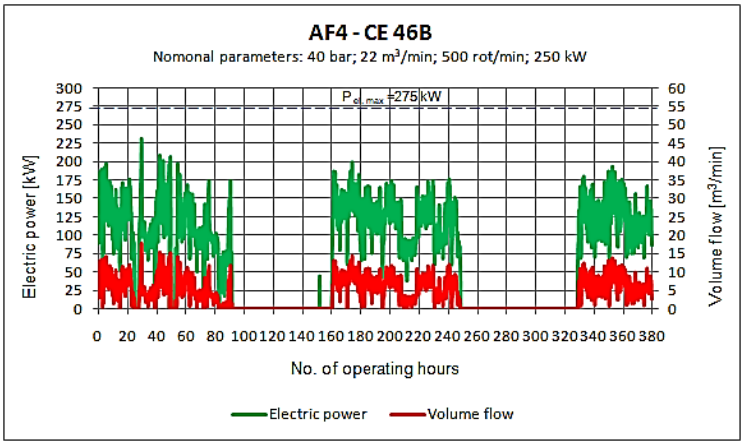

Fig. 7 Electric power and volume flow for compressor AF4-CE 46B

Based on the measured data, the losses and efficiencies of the compressors were determined according to the presented methodology, for the average operating regime corresponding to the monitored periods. The results are presented in Table 4.

Table 4

Parameters and efficiency at medium regime during the monitored period

No.	Parameter	Symbol.	Unit	Compressor type			
				AF1 CE 68B	AF2 CE 680B	AF3 CE 68B	AF4 CE 46B
1	Average volume flow	$\dot{V}_m$	m³/min	17.9	17.2	24.4	6.4
2	Compressor speed	n_r	rpm	520.0	540.0	520.0	500.0
3	Average power	P_a	kW	222.3	212.3	273.2	108.7
4	Theoretical power	P_t	kW	129.9	109.1	171.9	44.2

5	Throttling loses	P_{lam}	kW	24.4	23.4	33.3	8.6
6	Mechanical loses	P_m	kW	68.0	79.8	68.0	55.9
7	Compressor efficiency	η_c	%	58.4	51.4	62.9	40.6
8	El. motor efficiency	η_{me}	%	92.0	92.0	92.0	92.0
9	Total Efficiency	η_{mc}	%	53.7	47.3	57.9	37.3
10	Average load	S	%	49.4	38.6	60.7	43.5

The energy analysis of the compressor operation monitoring results is presented in table 6. The calculations were performed for the average power consumed, respectively the average flow produced during the operation periods. The periods when the compressors were switched off during the holidays, on non-working days or when the air flow of the compressors exceeded the consumer's requirement, were not considered.

Table 5 calculates the energy efficiency indices for the average operating regime.

Table 5

Compressor energy efficiency indices

No.	Parameter	Symbol	Unit	Compressor type			
				AF1 CE 68B	AF2 CE 680B	AF3 CE 68B	AF4 CE 46B
1	Compressor efficiency	η_c	%	58.4	51.4	62.9	40.6
2	Total efficiency	$\eta_{c,mot}$	%	53.8	47.3	57.9	37.4
3	Specific energy consumption *)	c	kWh/m^3	0.225	0.224	0.203	0.308

*) The air flow was considered at the suction conditions.

Table 5

Compressor energy analysis, at the average operating mode

No.	Parameter	Symbol.	Compressor type							
			AF1 CE 68B		AF2 CE 680B		AF3 CE 68B		AF4 CE 46B	
			kW	%	kW	%	kW	%	kW	%
	INTRARE									
1	Electric power	P_{el}	241.6	100.0	230.7	100.0	296.9	100.0	118.2	100.0
	IESIRE									
1	Theoretical power	P_t	129.9	53.8	109.1	47.3	171.9	57.9	44.2	37.4
2	Throttling losses	P_{lam}	24.4	10.1	23.4	10.1	33.3	11.2	8.6	7.3

3	Mechanical losses	P_m	68.0	28.1	79.8	34.6	68.0	22.9	55.9	47.3
4	Losses inside electric motor	P_{mel}	19.3	8.0	18.4	8.0	23.7	8.0	9.5	8.0
	TOTAL outputs		241.6	100.0	230.7	100.0	296.9	100.0	118.2	100.0

5. Results of monitoring electrical parameters

An ION7600 Class A type analyzer was installed in the general distribution board (GDB) of the compressor station, to monitor the parameters of the compressor power supply network. Recordings were made on the low voltage bars, with the recording of the average values of the electrical quantities at an interval of 10 minutes. The results of the recordings are shown in Figs. 8 ... 14.

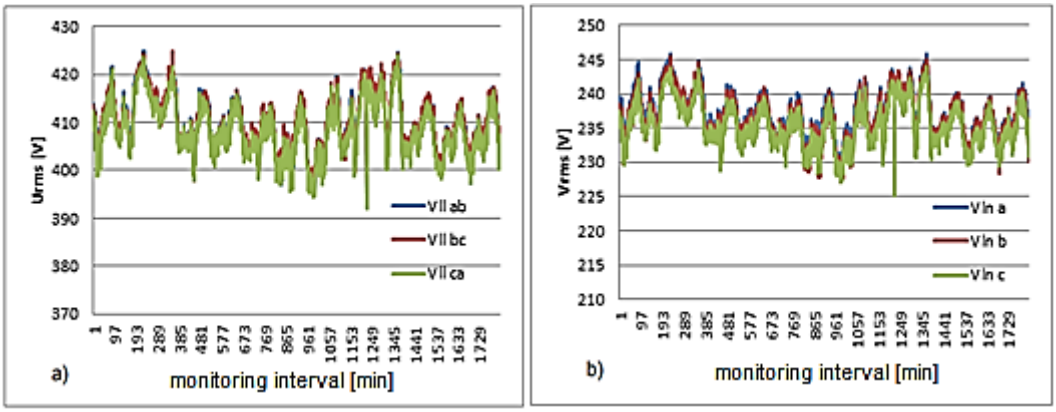

Fig. 8 Voltage variation at supply bars for GDB:
a - voltages between phases, U_{rms} [V]; b - phase voltages, V_{rms} [V]

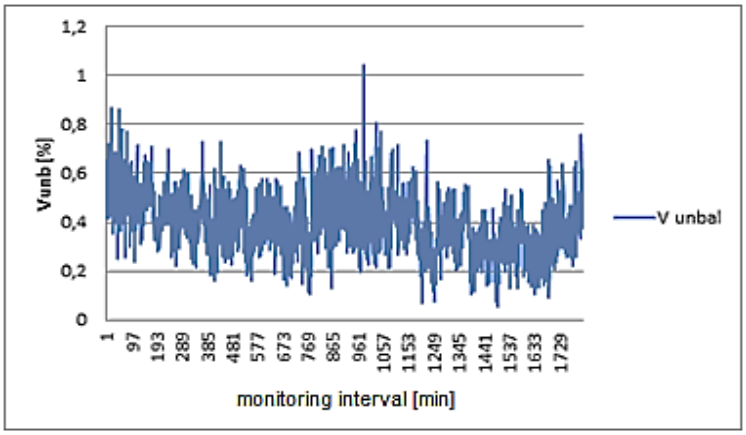

Fig. 9 Negative voltage asymmetry factor at GDB supply bars.

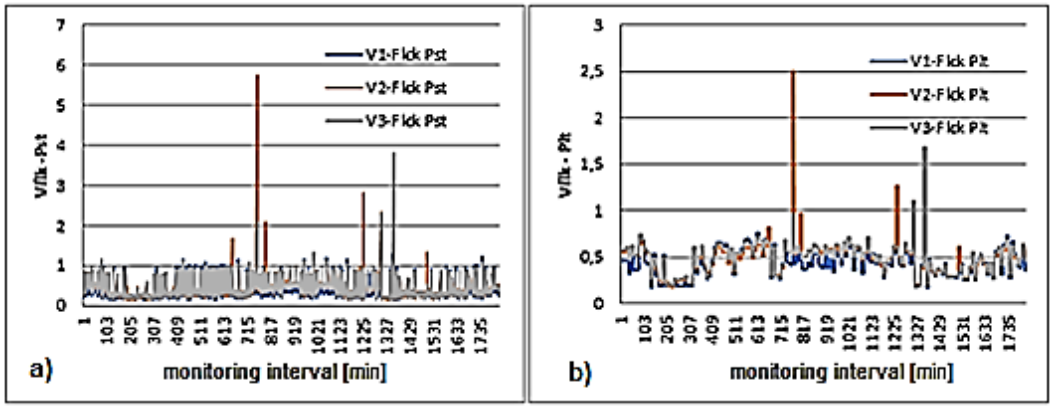

Fig. 10 Variation in the level of voltage fluctuations at the supply bars of the GDB.
a) Vflik-Pst level; b) Vflik-Plt level

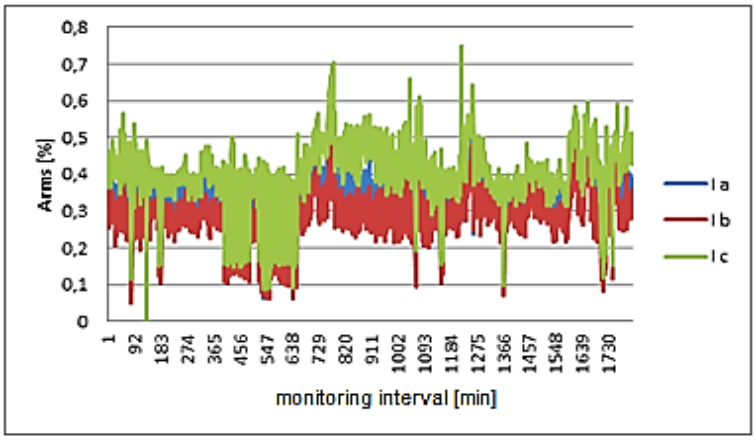

Fig.11 Electric current curve on the feed bar for GDB.

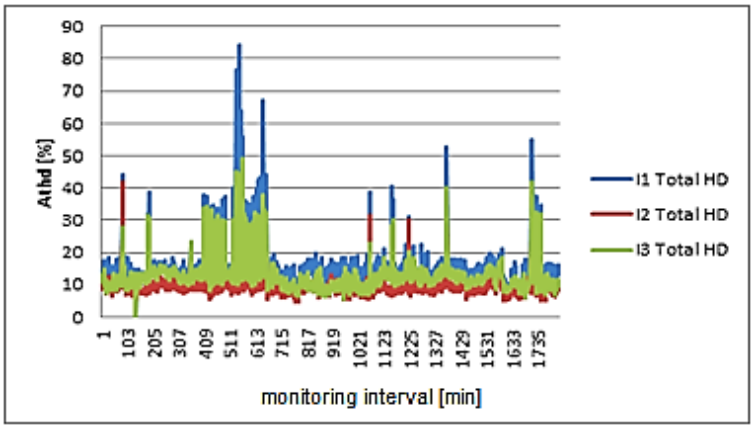

Fig.12 Electric current distortion factor
on supply phases a, b, c (THD I) - monitored values.

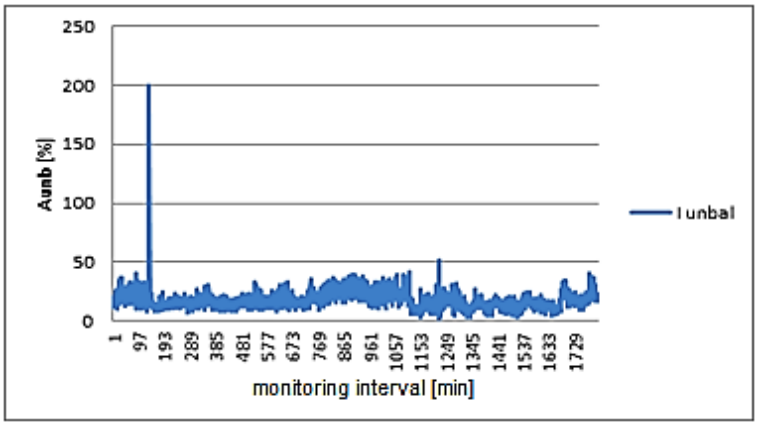

Fig. 13 Variation of negative current asymmetry factor for GDB.

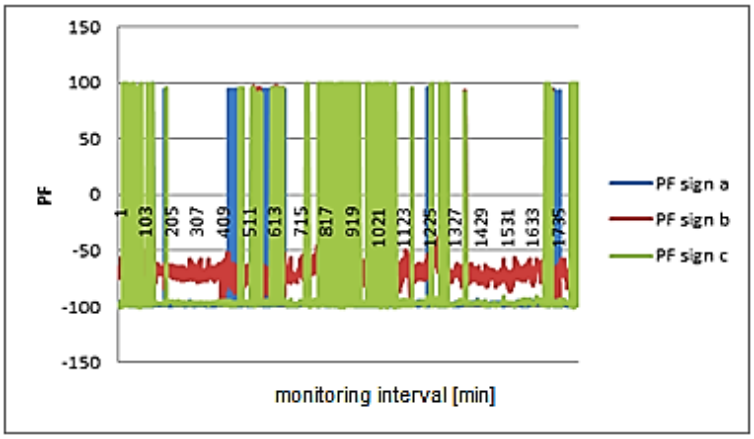

Fig. 14 Variation of power factor at feed bars for GDB on phases a, b, c.

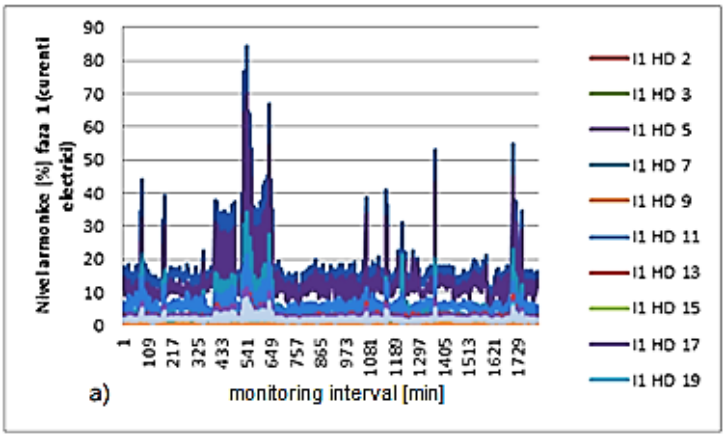

Fig. 15 The level of electric harmonics at the GDBsupply bars, a) Phase 1

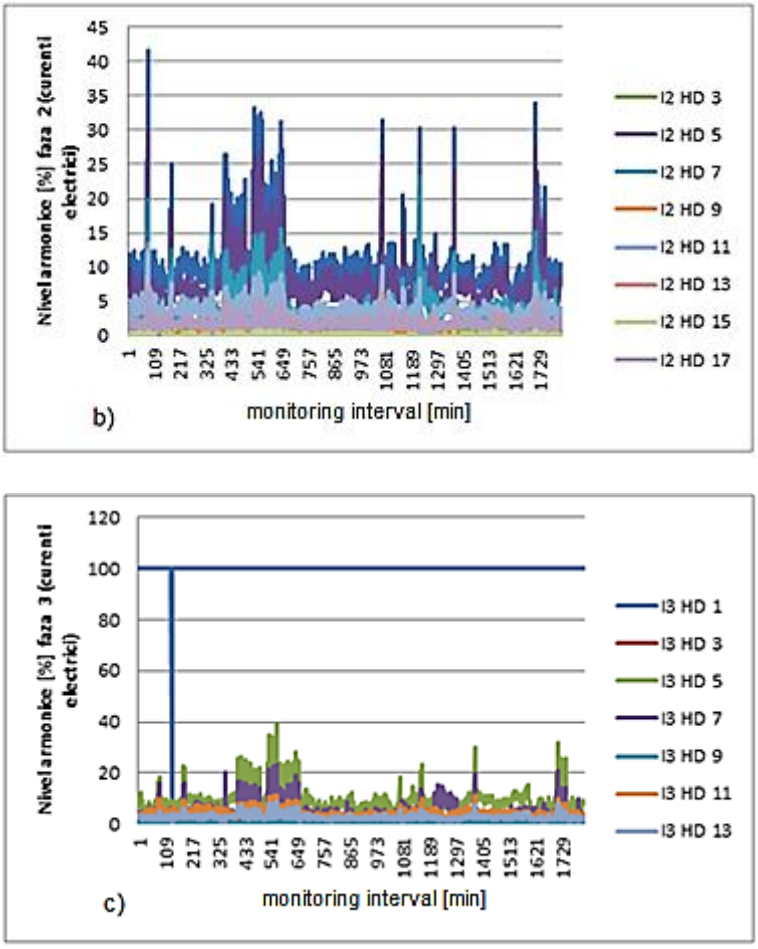

Fig. 15 The level of electric harmonics at the GDBsupply bars:
b) Phase 2; c) Phase 3

The voltage at the supply bars of the receivers shows variations: 225 ... 245.1 V voltage per phase and 392 ... 423.6 V voltage between phases, for GDB (Fig. 8), which must be within 230 ± 10% V and 400 ± 10% V respectively (207 ... 257 V/360 ... 440 V). Voltage fluctuations are recorded, accompanied by the flicker effect. The three phases are charged relatively symmetrically. It is noted that the values of the supply voltage during the measurements did not exceed the normal (normed) limit values. Fig. 9 shows the variation of the asymmetry factor during recording. It is found that the values of the negative asymmetry factor:

$$k_s = \frac{U^-}{U^+} 100 \ \ [\%] \tag{13}$$

where U^- is the negative sequence voltage (inverse) and U^+ is the positive sequence voltage (direct), does not exceed the range of allowable values of the negative asymmetry factor (<2%)[7], [8].

The analysis of the data in figure 10 shows that at the low voltage bars of the consumer supply system, in many cases the allowed levels of voltage fluctuations in the public network are exceeded ($P_{st\ allowed}$ = 0.9 and $P_{lt\ allowed}$ = 1.0). The number of events that lead to higher values than those allowed in the public network are small and are due to specific processes. In addition, in the energy system of other users, the allowed values are different from those in the public network, established according to the effects on the process carried out.

The data in Fig. 10 indicate that higher voltage variations occur in phase c, accompanied by a higher level of flicker indicators. It is noted that the curves P_{st} and P_{lt}, in the GDB, have almost the same shape. It is also found that, the level of the flicker (P_{st}, P_{lt}) is in the parameters normalized to the supply bars of the GDB [9], [10].

The electric currents on the three phases of the GDB have quite close values, however, indicating an asymmetric phase charge. The variations of these currents are shown in Fig. 11, and it is found that due to the high level of harmonics, it is necessary to adopt solutions to improve the shape of the electric current, for example by fitting appropriate filters [11], [12]. The total distortion factor of electric current - THD I, according to the shape of the curves in the graph shown in Fig. 12, indicates the sinusoidal shape of the current in the supply circuit. At a first comparison with the data on the level of distortion of the voltage on the bars, there is no direct influence, especially in the case of phase a, in which the harmonic distortion of the electric current is superior to the other two phases. It should be noted that the jumps in the variation curves of the harmonic spectrum are due to sudden variations in electric current at the start of various electrical equipment - motors (inrush current). These values are not specific for the analysis of harmonic distortion of electric current.

The variation of the electric asymmetry factor, during the recording time, is indicated in Fig. 13. The negative asymmetry factor was determined based on the relation:

$$k_s = \frac{I^-}{I^+} 100 \ \ [\%] \tag{14}$$

where I^- is the negative (reverse) sequence component of electric currents, and I^+ is the positive (direct) sequence component. The data in Fig. 13 show that, during the recording, the power asymmetry factor did not exceed the normal operating values, these being determined by the voltage asymmetry at the supply bars.

The variation of the power factor during the recording and in the time intervals in which the equipment was in operation is indicated in Fig. 14 for each phase. It is found that there is a significant circulation of reactive power in the supply circuit. It is necessary to check the reactive energy compensation installation and, if necessary, the local reactive energy compensation [13], [14].

The recorded values of the harmonic spectrum are affected specially by the specific operating mode, with frequent starts and stops of motors and other equipment. The real values of the harmonic spectrum can only be considered for stationary time intervals. Fig. 15 shows the values of the current harmonics on the three phases (a, b, and c) at the supply bars for GDB.

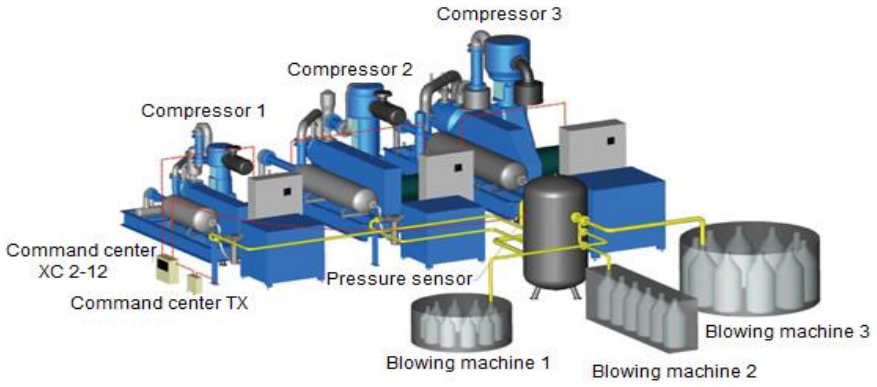

Fig.16 Electronic controlled compressor system of different capacities (Source: [15])

The examination of the operation of the compressor station found that there is no automatic management, on the principle of energy efficiency, of the mode of commissioning of the compressors, depending on the air flow required by the consumer. From this point of view, it appears necessary to implement an automatic management based on the system "EnergAir, Metacentre XC", recommended by the compressor manufacturer [15]. The energy control strategy consists in the realization of a system consisting of compressors with different flow rates and the commissioning of a group of compressors, selected so that, for the flow required by the consumer, they operate as close as possible to the rated load regime, which provides maximum efficiency. A possible arrangement for an electronic controlled compressor system of different capacities is shown in Fig. 16.

Fig. 17 shows the possible variants for grouping the four compressors AF1 ... AF4, according to the arrangement shown in Fig. 16, to achieve the required flow.

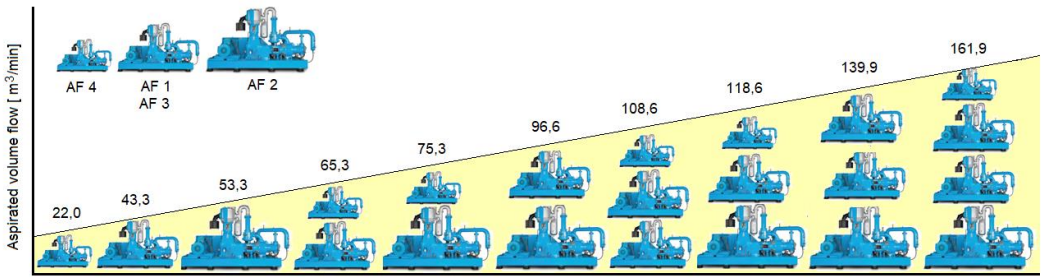

Fig.17. Grouping of compressors AF1 ... AF4 in relation to the required volume flow, according to the strategy of maximum energy efficiency.

The grouping is done automatically, the computer choosing which of the compressors will operate continuously at rated load, which will operate at partial load with flow control, and which are decommissioned. The implementation of such a system leads to very large savings on electricity consumed by compressors.

5. Conclusions

The energy analysis of the operation of the compressors reveals very low efficiencies, due to the operation at partial loads. As can be seen from Table 4, the average operating load was, for the monitored period, between 38.6% for AF2 CE-680B compressor and 60.7% for AF4-CE 46B compressor. This determined that the actual efficiency of the compressors was between 37.3% for the AF4–CE 46B compressor and 57.9% for the AF3–CE68B compressor. Compared to the maximum efficiencies, which correspond to the nominal load regime (Table 3), this means a decrease in energy efficiency by approx. 18%.

The heat resulting from the cooling of the compressors is not recovered, as it is discharged into the environment by means of an external cooling battery. From a thermodynamic point of view, by cooling the compressed air to ambient temperature, a heat flow equivalent to the power required for compression, is evacuated in ambient. Consequently, the recovery of this heat flow allows the increase of the general energy efficiency of the system by approx. 50%. Based on the energy analysis of compressor operation, the difference in electricity consumption per unit of aspirated flow at atmospheric conditions, between the mode of operation at rated load and the partial regime of about 50% found, is approx. 0.04 kWh /m^3.

For several 5000 operating hours per year, at an average flow of 65 m^3/min, observed during the monitored period, a possible electricity saving of at least 780 MWh/year results through such monitoring and management

of the mode of operation. For maximum efficiency, the system can be completed with a monitoring of the operation of the compressors, of SCADA type, which allows the centralized tracking of the use and the creation of a database on the operation history. An electronic system for managing the operation of compressors in relation to the required air flow, such as that shown in Figs. 18 and 17, may also be implemented. The main observations that emerge from the analysis of the electrical measurements performed are:

- there is a good framing of the voltage level on phases and between phases in the normed parameters (framing in the normed limits).
- there is an imbalance of the charge of the three phases of the analyzed electrical circuit.
- the power factor is correctly compensated (over 0.92).
- the level of electric harmonics is relatively high (it is noted that the 5-th and the 7-th electric harmonics, have very high values).

Under these conditions, to improve the quality of the power supply, it is necessary to charge the three phases in a balanced way, as well as to improve the compensation and the operation with an improved harmonic regime.

REFERENCES

[1] *PMB Plastic Bottle™* – https://plastic.bottle-manufacures.com

[2] *P. Baldowska-Witos, A. Tomporowski, W. Kruszelnicka, A. Idzikowski, K. Markowska* – Evaluation of the Quality of the Production Process PET Bottles – QPI, vol.1, iss.1, 2019, DOI 10.2478/cqpi-2019-0067.

[3] *W. Frank* - The Facts about PET, ILSI Europe Rep. Series - PET for food, update version 2017.

[4] *AF Compressors* – Product Catalog – www.afcompressors.com

[5] *N. Baran, S. Dimitriu, P. Raducanu, D. Stanciu, N. Boriaru, C. Ionita* – Bazele termodinamicii tehnice (The basics of engineering thermodynamics), vol 1-3, POLITEHNICA Press, Bucharest, 2010, ISBN: 978-606-515-046-1.

[6] *C. Stamatescu, D. Tasca, M. Grigoriu* – Compresoare volumice (Volumetric compressors), Editura Tehnica, Bucharest, 1965.

[7] *D. Enescu, A. Russo, R. Porumb, G. Seritan* - Dynamic Thermal Rating of Electric Cables: A Conceptual Overview. 2020 55th International Universities Power Engineering Conference (UPEC), 2020/9/1.

[8] *G. C. Lazaroiu, M. Roscia* - Definition methodology for the smart cities model, Energy Journal, Volume 47, Issue 1, Pages 326-332, Publisher Pergamon, 2012/11/1.

[9] *I. Pisica, G. Taylor, C. Chousidis, D. Thrichakis* - Design and Implementation of a Prototype Home Energy Management System. UPEC 2013, 48th Universities' Power Engineering Conference, 2013.

[10] *V.Pleşca, O. M. Ghiţă, I. M. Costea, C. K. Bănică, I. D. Mihalache, A. Neculiţă, L. D. Bănică* - Experiments on Extending the Flight Regimes of Electrically Powered Multi-Engine Drones Using Automatic Loading Systems. 2021 12th International Symposium on

Advanced Topics in Electrical Engineering (ATEE). Date Added to IEEE Xplore: 12 May 2021, DOI: 10.1109/ATEE52255.2021.9425251, Publisher: IEEE Conference Location: Bucharest, Romania, 25-27 March 2021.

[11] *C. Dumitrescu, I. Costea, O. Ghit, C. Banica* - Processing Images Obtained from UAVs for Preserving Contours in Order to Classify Shapes. 2021 12th International Symposium on Advanced Topics in Electrical Engineering (ATEE), 2021.

[12] *S. D. Grigorescu, C. Cepişcă, S. V. Paţurcă, O. M. Ghita, G. Seritan, F. Argatu, F. Adochiei, C. Banica* - Use of pedagogical agents to build multiple choice equations for an electric workshop based on LabVIEW, 2017 10th International Symposium on Advanced Topics in Electrical Engineering (ATEE), Conference Paper Publisher: IEEE 2017.

[13] *R. Somoghi, V. Purcar, E. Alexandrescu, I. C. Gifu, C. M. Ninciuleanu, C. M. Cotrut, F. Oancea, H. Stroescu* - Synthesis of Zinc Oxide Nanomaterials via Sol-Gel Process with Anti-Corrosive Effect for Cu, Al and Zn Metallic Substrates. Coatings 11 (4), 444, Jurnal Coatings Vol. 11, No. 4, pp 444, Multidisciplinary Digital Publishing Institute, 2021/4.

[14] *V. Geantă, I. Voiculescu, M. C. Cotrut, M. D. Vrânceanu, I. M. Vasile, J. C. Mirza Rosca* - Effect of Al on Corrosion Behavior in 3.5% NaCl Solution of AlxCoCrFeNi High Entropy Alloys. Conf., International Journal of Engineering Research in Africa, Vol. 53, pp 20-30, Trans Tech Publications Ltd, 2021.

[15] *METACENTRE – KB Sections* – https://support.metacentre.eu/portal/en/kb/metacentre